

Resistance-Demand Approach for Shear of High Strength Concrete Slender Beams

A.B. Shuraim¹, A. K. El-Sayed²

Abstract— The paper presents experimental shear tests of 18 beams tested with three main variables; the reinforcement ratio, the shear span to depth ratio, and the total depth of the beam. The paper introduces a novel approach in utilizing the knowledge about shear resistance degradation by coupling the shear resistance with the shear demand. Both the shear resistance and shear demand are correlated with flexural tensile strain from compatibility and equilibrium requirements. The basic shear strength, under a given loading is determined from the intersection of the demand and resistance curves. The procedure was verified against the results of the tested beams. It showed good prediction capability and can be useful to design practice.

Keywords—shear, concrete, beams, tests, resistance-demand

I. Introduction

Shear behavior in reinforced concrete beams is very complex where, the system becomes highly indeterminate transmitting shear through various mechanisms which are influenced by many parameters [ACI-ASCE-326, ACI-ASCE-426, ACI-ASCE-445 (2009)].

The traditional design of shear in most reinforced concrete design codes [ACI-318-2011, Eurocode 2-2004] is based on the assumption that the nominal strength is the summation of contributions of concrete and stirrups. The shear strength provided by concrete V_c is taken as the shear causing significant inclined cracking [ACI-318(2011)].

The shear causing significant inclined cracking in reinforced concrete beams is a key parameter in shear design. In slender beams without stirrups, the difference between inclined cracking shear and ultimate shear is not significant; however, for D-regions, the cracking shear is only a fraction of the ultimate shear. Most of the empirical equations tend to give the ultimate shear capacity of tested beams.

The concrete shear strength, V_c , is affected by the shear span to depth ratio; however, many semi-empirical equations do not include that effect as summarized in Table 1. Several multi-parameter empirical equations have been developed [Kim and Park 1996; Rebeiz 1999; Okamura and Higai 1980; and Zsutty 1968], however, shear empirical equations have been recognized to produce a large degree of scatter due to the scatter in test results and to the uncertainty in assessing the influence of complex parameters in a simple formula [ACI-ASCE-445, 2009].

Previous studies have indicated that shear strength in concrete beams decreases with increase in strain in the longitudinal reinforcement through various hypotheses [Vecchio and Collins, 1986; CSA Committee A23.3, 2004; AASHTO, 2008; Muttoni and Ruiz, 2008]. Another family of theoretical models relates concrete shear strength to the strain in the longitudinal reinforcement through various hypotheses

regarding the crack location, orientation and the state of strain or stress [Zararis and Papadakis, 2001; Tureyen and Frosch, 2003, Park et al, 2006]. Recent-ly, [Shuraim 2014] introduced an approach, which relates the shear strength capacity or shear resistance in a concrete beam with the internal shear resulting from applied load, thus termed as shear demand. The approach was found to produce a good predicting capability as verified against a database of 232 beams collected from 10 sources with a broad range of parameters [Shuraim (2014)].

This paper has two-fold objectives: first, it describes the experimental program for testing high strength reinforced concrete beams; second, briefly it describes the resistance-demand approach and examines its applicability to predict the shear strength of the tested beams. The test matrix is composed of 18 full-scale beams tested with three main variables; the reinforcement ratio, the shear span to depth ratio, and the total depth of the beam..

II. Experimental Program

A. Material characteristics

The target compressive concrete strength of the concrete used in the beams was 50-55 MPa after 28 days, which represents the lower category of HSC. The beams were constructed using concrete provided by a local ready-mix supplier. Table 2.1 gives the mix proportions of the concrete used in this study. Standard concrete cylinders 150×300 mm were cast during casting the beams and cured under the same conditions as the test beams. The average compressive strength at the time of beam testing, based on standard tests on concrete cylinders, ranged between 55.3 and 64.3 MPa.

Deformed steel bars were used in reinforcing the test beams. Steel bars with diameters of 12, 14, 18, and 20 mm were used as main tensile reinforcement while steel bars with diameter of 10 mm were used as top reinforcement. The actual tensile properties of the reinforcing bars were determined using standard tensile tests performed on three samples of each bar size. The actual properties of the bars are given in Table 1.

B. Specimen design

The A total of 18 full-scale reinforced concrete deep beams were constructed, nine of them with a total depth of 700 mm and the other nine with a total depth of 400 mm. three different reinforcement ratios, ρ , of 0.73, 1.21, and 1.83% were used and three different av/d ratios of 1, 1.5, and 2. Cross sections and longitudinal reinforcement are as shown in Figure 2

¹ Professor of civil Engineering, King Saud University, Saudi Arabia

2 Associate Professor of civil engineering, King Saud university

Table I: Reinforcement data

Bar diameter (mm)	Yield strength (MPa)	Ultimate strength (MPa)	Modulus of elasticity (GPa)
10	533	765	195
12	569	658	207
14	565	671	183
18	546	671	179
20	542	666	179

Table II: Concrete mix proportions

Water-cement ratio	0.37
Water, kg/m ³	167
Cement content, kg/m ³	450
Fine aggregate content, kg/m ³	787
Coarse aggregate size, mm	9.5 to 19
Coarse aggregate content, kg/m ³	971
High-range water-reducing admixture, L/m ³	3
Air, %	2
Slump, mm	140

As the anchorage of the longitudinal bars is one of the critical details affecting the behavior of deep beams, the ends of the longitudinal bars of such beams were provided with 90-degree standard hooks. All beams had overhang length of 252 to 388 mm beyond the supports on each side as anchorage length for the reinforcing steel to avoid premature bond failures prior to shear failures. In addition, both overhangs behind the supports were provided with 8mm-diameter steel stirrups (3 stirrups each) to enhance the bond behavior and to fix the longitudinal bars in their positions. No stirrups were included within the shear span of the beams between the point load and supports. The details of the test specimens are given in Table III and shown in Figure 1 and Figure 2.

The designation of the beams uses the character B standing for beam and the first number 700 or 400 refers to the beam depth. The second number (1 to 5) stands for a_v/d ratio. The third number 50 refers to the concrete strength and the character r1, r2, and r3 refers to the reinforcement ratio of 0.73, 1.21, and 1.83%, respectively.

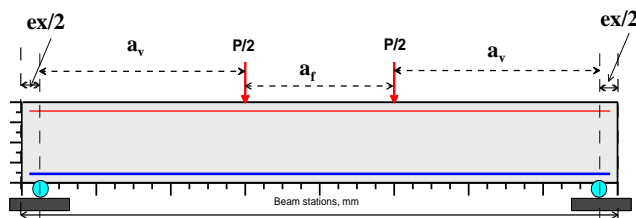


Figure 1: Typical tested beam notations

Table III: Tested beam data and results.

Beam	f'_c	h , d (mm)	a_v/d	ρ	Sec. #	V_u (kN)
B700-5-50-r1	65.9	700 612	5	0.73	1	105
B700-5-50-r2	65.9	700 612	5	1.21	2	130
B700-5-50-r3	65.9	700 612	5	1.83	3	143
B700-4-50-r1	65.9	700 612	4	0.73	1	106
B700-4-50-r2	65.9	700 612	4	1.21	2	140
B700-4-50-r3	65.9	700 612	4	1.83	3	162
B700-3-50-r1	65.9	700 612	3	0.73	1	116
B700-3-50-r2	65.9	700 612	3	1.21	2	156
B700-3-50-r3	65.9	700 612	3	1.83	3	204
B400-5-50-r1	59	400 335	5	0.74	5	68
B400-5-50-r2	59	400 335	5	1.22	6	77
B400-5-50-r3	59	400 335	5	1.82	4	108
B400-4-50-r1	59	400 335	4	0.74	5	78
B400-4-50-r2	59	400 335	4	1.22	6	108
B400-4-50-r3	59	400 335	4	1.82	4	122
B400-3-50-r1	59	400 335	3	0.74	5	104
B400-3-50-r2	59	400 335	3	1.22	6	130
B400-3-50-r3	59	400 335	3	1.82	4	138

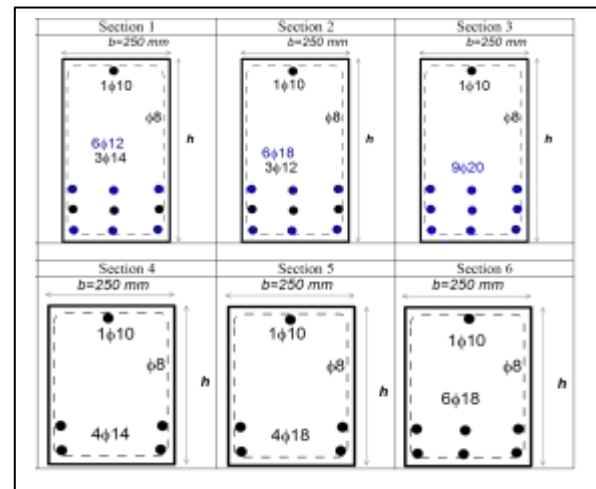


Figure 2: Typical cross-sections of beams

III. The Proposed Procedure

The design procedure developed earlier [Shuraim, 2014] involves two elements. First, shear resistance relationship which express the shear degradation as a function of the longitudinal strain in the bottom reinforcement, among other variables. Second, shear demand relationship which represents the required shear as the applied load increases, and also can be expressed as a function of the longitudinal strain in the bottom reinforcement. Typical curves are shown in Figure 3.

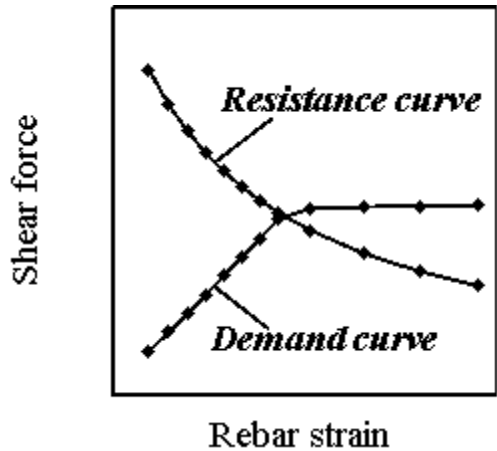


Figure 3: Typical shear resistance and demand curves.

A. Shear versus strain relationship

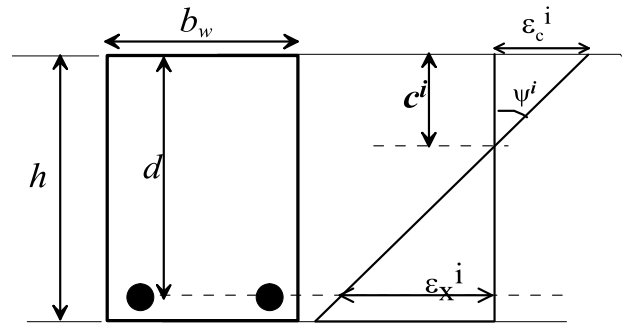
The shear resistance-longitudinal strain relationship is expressed as follows:

$$V_R^i = \frac{0.63}{1+500 \epsilon_s^i} (f_c')^{\frac{1}{3}} b_w d \quad (1)$$

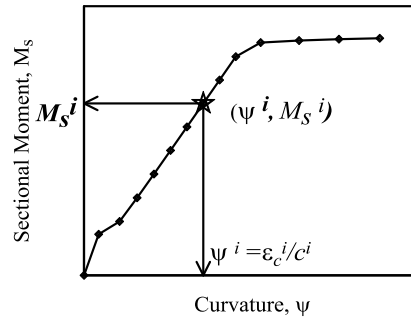
where, f_c' is the concrete compressive strength, b_w is the beam width, and d is the effective depth of the bottom reinforcement. Finally, the longitudinal strain is expressed as follows with reference to Figure 4.

$$\epsilon_s^i = \psi^i d - \epsilon_c^i \quad (2)$$

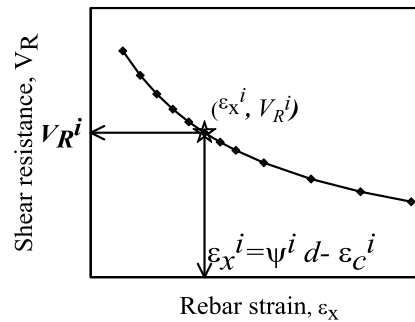
Figure 4 (a) shows a linear strain distribution in a typical reinforced concrete cross section of a simple beam under arbitrary static loading. ϵ_c^i is the compressive strain at the top layer while c^i is the depth of the neutral axis measured from the compression face. Under such assumptions, the curvature, $\psi^i = \epsilon_c^i / c^i$. Figure 4(b) shows typical moment-curvature relationship that can be developed in incremental form by increasing the top strain ϵ_c^i , and adjust the neutral axis depth in order to satisfy equilibrium, from which the associated sectional moment, M_S^i , is obtained. The results of ϵ_c^i , ψ^i and M_S^i are to be tabulated in order to compute ϵ_s^i , V_R^i , as per Eqs. (1 and 2).



(a)



(b)



(c)

Figure 4: Schematic steps for developing shear resistance curve.

B. Shear demand curve

For a simply supported beam subjected to two concentrated loads, V_D^i , at a shear span, a_v , the internal shear force and moment diagrams are as shown in Figure 5. The shear demand that is associated with a particular shear resistance and longitudinal strain, ϵ_s^i , is computed from M_S^i and a_v , such that:

$$V_D^i = M_S^i / a_v \quad (3)$$

Repeating the process for a sufficient number of concrete top strains such that ($\epsilon_c^0 \leq \epsilon_c^i \leq \epsilon_c^u$) is to be performed in order to generate the demand and resistance curves (ϵ_s^i , V_D^i , V_R^i).

Therefore, for any top strain value, ϵ_c^i , the associated values for ψ^i and M_S^i , ϵ_s^i , V_R^i , and V_D^i become readily

available. The next step is to graph the V_R^i , and V_D^i versus the strain as shown in Figure 6, where the shear demand follows an ascending path while the shear resistance follows a descending path. Their intersection point defines the basic shear strength, V_{RD} , for a normal size beam without stirrups.

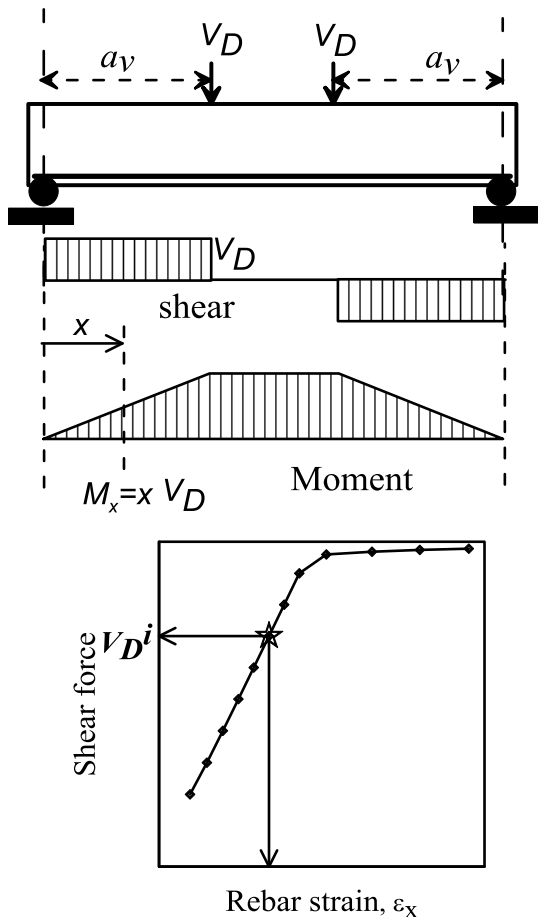


Figure 5: Schematic steps for developing shear demand curve.

C. Size effect factor

Studies (ACI-ASCE Committee 445, 2009) have shown that there is a very significant size effect or depth of member effect on the shear strength of members without transverse reinforcement where the average shear stress to cause failure decreases with the increase of the effective depth. Several models have been proposed in the literature, among them those shown in Table 1. This study adopts a size reduction factor following CSA A23.3-2004 with a slight modification. The size factor is to modify the basic shear strength in Eq. (20), such that:

$$V_c = \begin{cases} V_{RD} & , \quad h \leq 400 \text{ mm} \\ \frac{1200}{800 + h} V_{RD}, & h > 400 \text{ mm} \end{cases} \quad (4)$$

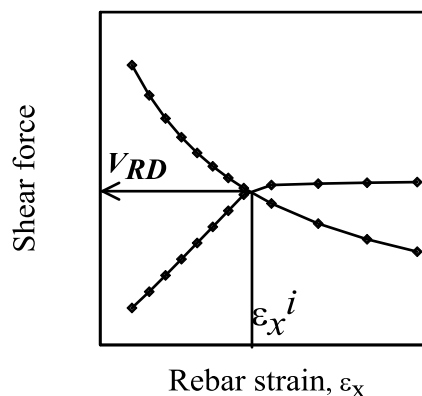


Figure 6: Defining basic shear- the intersection of the resistance and demand curves.

IV. Comparisons with Test Results

The experimental shear strength and the computed shear strength for the 18 tested beams are presented in

Figure 7 through Figure 9.

Figure 7 shows results for beams with $a_v/d=3$. It is to be noted that labels 730 and 430 refers to beam depths of 700 mm and 400 mm, respectively, at shear span of three. Similar notations are used in Figure 8 Figure 9. The shear strength is presented against the flexural reinforcement ratio and it is observed that the shear increases linearly with the increase in reinforcement ratio. The same trend is observed both experimentally and by the analytical procedure for all shear span to depth ratios. In the RD formulation, the effect of reinforcement ratio takes place through the sectional moment, M_s .

Numerically, the ratios of V_c/V_{test} for 700 mm-beam beams have a mean value of 1.05, a standard deviation of 0.09 and a CoV of 8.35 percent. For 400-mm beams, the mean value is 0.96, with standard deviation of 0.10 and a CoV of 10.05 percent. This represents a good prediction, especially since it produced a low scatter and a mean value within 5 percent.

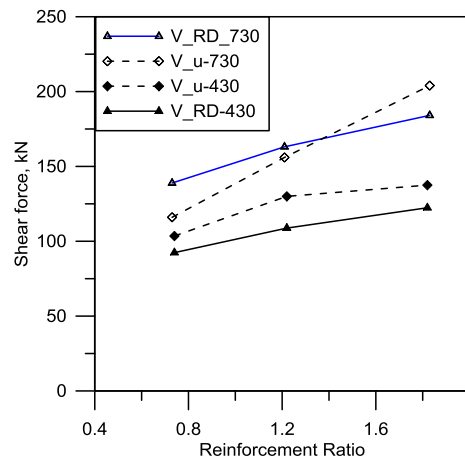


Figure 7: Shear strength for beams with $a_v/d=3$

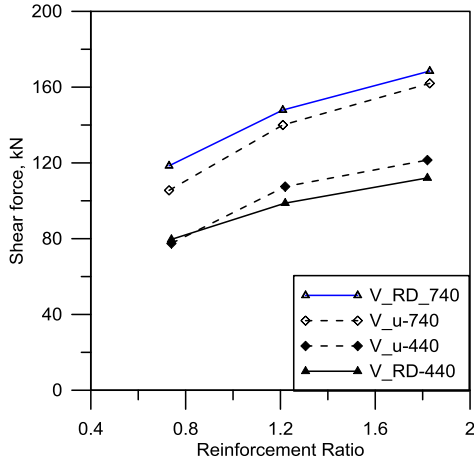


Figure 8: Shear strength for beams with $a_v/d=4$.

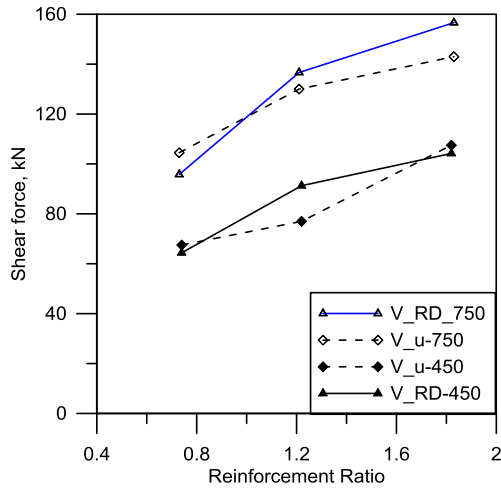


Figure 9: Shear strength for beams with $a_v/d=5$.

V. CONCLUSIONS

The paper presented a rational design procedure for computing the concrete shear contributions, V_c . The procedure was utilized to assess the experimental results for the 18 tested beams. The performance of the procedure in predicting the shear strength represents good capability in terms of magnitude and trend, thus, it can be used for design purpose.

Acknowledgment

This work was supported by NSTIP strategic technologies program number (ADV-1023) in the Kingdom of Saudi Arabia

References

- [1] Joint ACI-ASCE Committee 326(1962). Shear and diagonal tension, ACI Journal, 59(1): 1-30.
- [2] Joint ACI-ASCE Committee 426(1987). The shear strength of reinforced concrete members, Part 4 of ACI Manual of Concrete Practice, ACI, Farmington Hills, MI, 111 pp.
- [3] Joint ACI-ASCE Committee 445 (Reapproved 2009). Recent Approaches to Shear Design of Structural Concrete, ACI Manual of Concrete Practice, ACI, Farmington Hills, MI, USA, 56 pp.
- [4] ACI-318 (2011). Building Code Requirements for Structural Concrete (ACI 318-08) and Commentary, ACI, Farmington Hills, MI, USA, 510 pp.
- [5] Eurocode 2(2004). Design of Concrete Structures, Part 1-1: General Rules and Rules for Buildings (EN1992-1-1), European Committee for Standardization, Brussels, Belgium, 230 pp.
- [6] Kim, J-K, and Park, Y-D(1996). Prediction of Shear Strength of Reinforced Concrete Beams without Web Reinforcement, ACI Materials Journal, 93(3): 213-222.
- [7] Rebeiz, K. S.(1999). Shear strength prediction for concrete members, Journal of Structural Engineering, ASCE, 125(3): 301-308.
- [8] Okamura, H., and Higai, T. (1980). Proposed Design Equation for Shear Strength of R.C. Beams without Web Reinforcement, Proceedings, Japan Society of Civil Engineering, 300:131-141.
- [9] Zsutty, T. C. (1968). Beam shear strength prediction by analysis of existing data, ACI Journal, 65(11): 943-951.
- [10] Vecchio, F. J., and Collins, M. P.(1986). The Modified Compression Field Theory for Reinforced Concrete Elements Subjected to Shear, ACI Journal, 83(2): 219-231.
- [11] CSA Committee A23.3 (2004). Design of Concrete Structures, Canadian Standards Association, Mississauga, Ontario, Canada, 214 pp.
- [12] AASHTO. (2008). AASHTO LRFD Bridge Design Specifications, American Association of State Highway and Transportation Officials.
- [13] Muttoni, A., and Ruiz, M. F.(2008). Shear Strength of Members without Transverse Reinforcement as Function of Critical Shear Crack Width," ACI Structural Journal, 105(2): 163-172.
- [14] Zararis, P. D., and Papadakis, G. Ch.(2001). Diagonal shear failure and size effect in RC beams without web reinforcement, Journal of Structural Engineering, ASCE, 127(7): 733-742.
- [15] Tureyen, A. K., and Frosch, R. J. (2003). Concrete Shear Strength: Another Perspective, ACI Structural Journal, 100(5): 609- 615.
- [16] Park, H-G, Choi, K-K, and Wight, J. K.(2006). Strain-Based Shear Strength Model for Slender Beams without Web Reinforcement, ACI Structural Journal, 103(6): 783-793.
- [17] Shuraim, A. B., (2014), "A Novel Approach for Evaluating the Concrete Shear strength in Reinforced Concrete Beams," Latin American Journal of Solids and Structures, Vol. 11, No. 1, pp. 93-112.